Polymer 263 (2022) 125511

Contents lists available at ScienceDirect

Polymer

journal homepage: www.elsevier.com/locate/polymer

Effect of compatibilizer addition on the surface nucleation of dispersed polyethylene droplets in a self-nucleated polypropylene matrix

Sebastián Coba-Daza [a,d], Enrico Carmeli [d], Itziar Otaegi [a], Nora Aranburu [a], Gonzalo Guerrica-Echevarria [a], Sussane Kahlen [d], Dario Cavallo [c,*], Davide Tranchida [d,**], Alejandro J. Müller [a,b,***]

[a] POLYMAT and Department of Advanced Polymers and Materials: Physics, Chemistry and Technology, Faculty of Chemistry, University of the Basque Country UPV/EHU, Paseo Manuel de Lardizabal 3, 20018, Donostia-San Sebastián, Spain
[b] IKERBASQUE, Basque Foundation for Science, Plaza Euskadi 5, Bilbao, 48009, Spain
[c] Department of Chemistry and Industrial Chemistry, University of Genova, Via Dodecaneso, 31, 16146, Genova, Italy
[d] Borealis Polyolefine GmbH, Innovation Headquarters, St. Peterstrasse 25, 4021, Linz, Austria

ARTICLE INFO

Keywords:
Compatibilization
Surface nucleation
Self-nucleation
Supernucleation
Polypropylene
Polyethylene

ABSTRACT

A significant portion of the global plastics market encompasses the production of polyolefin materials and especially polypropylene (PP) and polyethylene (PE), as commodity polymers with a wide range of applications. However, the increase in the generation of unsustainable plastic waste requires a close technological look-up to address this challenge adequately. In this context, mechanical recycling is part of the strategies expected to contribute to the solution. Nevertheless, the melt blending process presents a challenge due to the immiscibility between PP and PE. Therefore, compatibilization strategies are meant to solve the problem effectively. In this paper, we employ a commercial ethylene-*ran*-methyl acrylate random copolymer as a compatibilizer for PP/PE blends. With the addition of the compatibilizer, it was possible to obtain a 44% reduction in PE domain size, while ductility increased by around ~40% with respect to uncompatibilized blends. Interesting results were obtained concerning the crystallization behavior of the blends. The overall isothermal crystallization kinetics of the different blend components was studied, and a synergistic nucleation effect of the PP and the compatibilizer toward the PE phase was found. For the first time, the effect of the compatibilizer on the surface nucleation of PE in a self-nucleated PP matrix phase is reported. An enhancement in the crystallization rate of PE was found when the self-nucleation protocol was applied to the polypropylene matrix phase for neat and compatibilized blends. The nucleation efficiency was in the range of 120–124%, indicating a *supernucleation* behavior. The induced crystallization at the interface by the self-nucleated polypropylene is the reason for such high nucleation efficiencies. Surprisingly, a higher amount of compatibilizer decreases the overall crystallization rate of PE droplets. The compatibilizer segregates at the interface between both polymers, reducing the surface nucleation of the PE droplets on the PP matrix phase. The results presented in this paper lead the way toward improving the use of post-consumer recycled materials.

1. Introduction

Blending polymers is a versatile and inexpensive way to control the performance of polymeric systems [1]. Blends are generally composed of two or more polymers and often contain compatibilizers or fillers. The blending process, specifically in the case of isotactic polypropylene (PP) and polyethylene (PE), is intended to simulate the post-consumer recyclate (PCR) composition of sorted materials. These two polymers are commodities in the worldwide plastic market, and since they are not biodegradable, they represent a challenge in the recycling field [2]. In

* Corresponding author.
** Corresponding author.
*** Corresponding author. POLYMAT and Department of Advanced Polymers and Materials: Physics, Chemistry and Technology, Faculty of Chemistry, University of the Basque Country UPV/EHU, Paseo Manuel de Lardizabal 3, 20018, Donostia-San Sebastián, Spain.
E-mail addresses: dario.cavallo@unige.it (D. Cavallo), davide.Tranchida@borealisgroup.com (D. Tranchida), alejandrojesus.muller@ehu.eus (A.J. Müller).

https://doi.org/10.1016/j.polymer.2022.125511
Received 17 June 2022; Received in revised form 12 October 2022; Accepted 6 November 2022
Available online 14 November 2022

this context, blending PP and PE allows us to understand their reuse in high-demand applications and favors the sustainable development of the plastic market [3]. Despite having similar properties, PP and PE are immiscible; therefore, the final properties of the blended material are inferior to the bulk properties of the single components. Generally, when immiscible polymers are mixed in the melt, the minor component is dispersed in droplets within the matrix formed by the major blend component, and, given the high interfacial tension, coalescence of the dispersed phase is promoted [3]. Consequently, large particle sizes are obtained, and the stress transfer is deficient at the interface, resulting in poor final mechanical properties.

The enhancement in the properties of blended materials caused by the addition of a compatibilizer has been studied in the literature [4–7]. Reduction in interfacial tension leads to a finer morphology. The interaction between the compatibilizer and the two distinct polymeric phases avoids or reduces the coalescence of the dispersed phase during blend preparation [8,9]. Hence, a compatibilizer can reduce the average particle size and its dispersion (i.e., reducing the width of the particle size distribution). The generation of a finer morphology directly affects the mechanical properties because the stress transfer between the phases is more homogeneous, and the stress concentration at the interface is reduced, preventing early crack initiation at the interface [6]. For example, Fortelný et al. [10] studied the effect of adding ethylene-propylene-diene rubber (EPDM) to a polypropylene/low-density polyethylene (PP/LDPE) blend, obtaining a remarkable increment in the impact strength with 5 wt% of EPDM.

Additional studies with copolymers and nanofillers have also been reported by Su et al. and Graziano et al. [11,12]. They discuss the enhancement of mechanical properties and the crystallization characteristics of PP/PE blends by adding PP-graft maleic anhydride (PP-*g*-MA) with silica nanoparticles. The addition of such components increases the compatibility between phases and improves elongation, tensile moduli, and strength. Recent studies using specific copolymer designs have been reported. For example, Klimovica et al. [13] used grafted PE-*g*-PP copolymers in different graft lengths to promote the compatibilization of PE/PP blends. The results show an efficient compatibilizing effect of the grafted polymer due to its specificity toward each polymer phase, thus decreasing the interfacial tension and improving the mechanical properties.

In immiscible blends of two semi-crystalline polymers, the addition of a compatibilizer can have different effects on the crystallization of the phases, whether it consists of a non-reactive or a reactive compatibilization process. In the case of non-reactive compatibilization, the effects are generally small [14,15] because the two phases crystallize independently. One of the reported effects is the migration of heterogeneities from one phase to the other, causing reductions or increases in the nucleation of the respective phase [16]. In the case of reactive compatibilization, a general decrease in the degree of crystallinity has been reported in polyamide/low-density polyethylene (PA6/LDPE) systems in the works of Scaffaro et al. and Macosko et al. [15,17] because as the reactive process occurs, the chains located near the interface are grafted onto the polymers, thus losing mobility [14]. Adding molecules containing highly reactive functional groups can generate chemical interactions between the polymer components during melt blending. This is the case of adding maleic anhydride (MA) to the PP/PA systems [18]. The MA is grafted to the PP and simultaneously can react with the amino group present in the PA chain, producing a polypropylene-*grafted*-polyamide segment at the interface [19,20]. It is also important to mention that in many cases, reactive compatibilization induces fractionated crystallization in some polymer blends [15,21,22]. For example, Yordanov et al. [23] investigated the addition of different types of compatibilizers in the LDPE/PA6 blend system. They were able to quantitatively identify the amount of PA6 droplets with a diameter lower than a determined critical diameter, as well as the dependence of fractionationated crystallization importance from the use of one or other compatibilizers, such as polyethylene functionalized with acrylic acid (EAA), and Styrene-ethylene-butylene-styrene grafted with maleic anhydride (SEBS-*g*-MA).

During polymer crystallization, nucleus formation is the first step from a supercooled liquid to a semi-crystalline material [24]. This step is followed by crystal growth [25]. Understanding both processes is crucial, although they are not easy to study independently. Some strategies have been used to study only nucleation, which consists of confining the polymer in very small domains (in the order of micro or even nano-domains) within a matrix acting as an inert medium [26–28]. With this strategy, the overall crystallization process can be dominated by primary nucleation because crystals can quickly grow and fill the volume of each droplet, and therefore, the growth contribution to the overall crystallization rate is negligible. In this case, the overall kinetics of crystallization tends to be a first-order process (that is, dominated by nucleation) [29].

Self-nucleation (SN) is a thermal treatment for injecting a high number of active self-nuclei into a polymer melt [30]. When this thermal protocol is applied, the nucleation density is expected to increase exponentially when self-nuclei are produced. Self-nuclei are produced during the melting of the material, and they are considered the best nucleating agent for the polymer since they have the same chemical structure and crystal lattice as the crystallizing polymer. In particular, if the self-nucleation temperature is low enough, crystal fragments (self--seeds) are left in the polymer melt. Thus, the presence of self-nuclei or crystal fragments in the melt can promote epitaxial nucleation [30]. A recent study by our group [22] observed an enhancement of the crystallization kinetics of PE-dispersed droplets in PP/PE blends when the self-nucleation protocol was applied to the PP matrix phase. Therefore, it was reported that the surface-induced nucleation of PE occurs through epitaxial growth on top of previously self-nucleated and annealed PP crystals, a well-known case of polymer-polymer epitaxy [24].

In the context of compatibilized polymer blends, the self-nucleation protocol allows for studying the effect of adding a compatibilizer on the nucleation process of the lower melting phase. To the best of our knowledge, the study of the thermal properties in a polypropylene/polyethylene/compatibilizer system using self-nucleation has not previously been reported.

In the present paper, we investigate the effect of different compatibilizer contents on the mechanical, thermal, and morphological properties of PP/PE blends. Thermal characteristics were tackled with two main approaches: using standard heating-cooling-heating scans and isothermal crystallization kinetics and following the novel method for the analysis of surface-induced crystallization in semi-crystalline polymer blends [24].

2. Experimental section

2.1. Materials

Borealis Polyolefine GmbH kindly supplied the employed polymers. Isotactic polypropylene with PVCH nucleating agent (HD905CF, Melt Flow Rate (MFR) (230 °C/2.16 kg) = 6.5 g/10 min) and polyethylene (FB1350, MFR (190 °C/21.6 kg) = 15 g/10 min, density 935 kg/m^3) were used to produce the blended materials in a 70/30 wt% composition. A compatibilizer agent, an ethylene-methyl-acrylate copolymer from BOREALIS and named here as COMP, was used in different proportions (10 and 20 wt% with respect to the dispersed phase content) to study the thermal behavior, as well as the effect on mechanical properties and morphology. The blends were prepared by melt compounding in a COLLIN ZK25 co-rotating twin-screw extruder-kneader with a constant temperature of 200 °C at 200 rpm (D = 25 mm and L/D = 30). The injection molding process (BATTENFELD BA230E; D = 18 mm and L/D = 17.8 mm) was used to obtain tensile (ASTM D638, type IV, thickness 2 mm) and impact (ASTM D256, thickness 3.2 mm) specimens. The codes assigned to the blends are as follows: PP/PE 70/30 for the blend with 70 wt% of PP and 30 wt% of PE. In the compatibilized blends:

PP/PE/COMP 70/30/3 and PP/PE/COMP 70/30/6, where 3 and 6 represent 10 and 20 wt% with respect to the dispersed phase (PE) content, respectively.

2.2. Methods

2.2.1. Scanning electron microscopy analysis

Morphological characteristics of the blended materials were acquired in a HITACHI TM3030Plus Tabletop Scanning Electron Microscope (SEM) at 15 kV. Before observation, the samples were cryogenically fractured and etched in a solution containing 1.3 wt% potassium permanganate ($KMnO_4$); 32.9 wt% phosphoric acid (H_3PO_4), and 65.8 wt% of sulfuric acid (H_2SO_4) as proposed by Aboulfaraj et al. [31] for the observation of the lamellar morphology. Finally, the samples were gold-coated in an SC7620 Mini Sputter Coater (Quorum).

2.2.2. Differential scanning calorimetry and isothermal crystallization kinetics

Samples weighing approximately 5 mg were placed in aluminum pans and tested under an ultra-high purity N_2 atmosphere in a PerkinElmer DSC 8000. The equipment was calibrated with indium and tin standards. Differential scanning calorimetry (DSC) data were analyzed with PerkinElmer Pyris software. Standard heating-cooling-heating DSC measurements were employed for this purpose. The first heating was carried out from 25 to 200 °C at 20 °C/min. The samples were kept for 3 min at that temperature to erase the thermal history, and then a cooling step down to 0 °C at 20 °C/min was performed. Finally, samples were heated up to 200 °C, also at 20 °C/min.

In the isothermal crystallization kinetics study, measurements were done using the method recommended by Lorenzo et al. [32]. For the matrix phase (PP), see Fig. 1a: (1) samples were heated at 200 °C and (2) kept at that temperature for 3 min to erase thermal history; (3) a cooling step at 60 °C/min to the chosen isothermal crystallization temperature (T_c) was performed; (4) the samples were held at T_c for enough time to allow the crystallization process to reach saturation; (5) a heating scan from T_c to 200 °C at 20 °C/min was applied. The lowest T_c value was chosen as the minimum temperature where crystallization during cooling at 60 °C/min could be avoided, see Ref. [33].

For the dispersed phase (PE), see Fig. 1b: Steps (1) and (2) are the same as above; (3) the samples were cooled down to 25 °C at 20 °C/min to produce a standard crystalline state; (4) a heating scan was performed to a temperature where the matrix phase (PP) remains in the crystalline state while the dispersed phase (PE) is in the melt (150 °C in this case); (5) the samples were kept at 150 °C for 5 min; (6) a cooling scan to the isothermal crystallization temperature was performed for the PE phase at 60 °C/min; (7) samples were held at T_c for enough time for the crystallization process to reach saturation; (8) final heating scan from T_c to 150 °C at a rate of 20 °C/min was done to study the melting behavior of the dispersed phase.

2.2.3. Self-nucleation thermal protocols

Two thermal protocols were applied to study the enhancement of the crystallization rate of the polyethylene dispersed phase. Self-nucleation of the polypropylene in the matrix phase was applied before following the crystallization of the dispersed phase via non-isothermal and isothermal runs.

The protocol for the self-nucleation of the PP matrix phase (or the PE minor phase) is the one devised by Fillon et al. [33] and reviewed by Michell et al. [33] and more recently by Sangroniz et al. [34]. It includes six steps carried out at 10 °C/min. Fig. S1 in the supplementary information describes the process, which briefly consists of the following steps:

1. The sample was heated up to 225 °C and held at that temperature for 5 min to remove the previous thermal history.
2. The material was cooled to 20 °C to create a "standard" crystalline state.
3. The sample was heated to a temperature called T_s^{PP} (Self-nucleation temperature of the PP phase).
4. The material was kept at T_s^{PP} for 5 min to promote the production of different crystalline states of the matrix as follows: (a) if the used T_s^{PP} is higher than the melting point (T_m) of the PP and does not produce any change in the crystallization temperature (T_c), the material is in *Domain I*; (b) if the T_s^{PP} used can melt most of the crystals (or all of them but at a temperature just above the end melting temperature), but crystal fragments (self-seeds) or residual order in the melt (melt memory effects) that can act as self-nuclei remain, the material is within *Domain II*; (c) when partial melting causes the annealing of the remaining crystals in the 5 min treatment at T_s^{PP}, the material is in *Domain III*.

In the matrix phase: *Domain I* was found between 225 °C and 167 °C, *Domain II* was detected from 164 °C to 166 °C, and finally, *Domain III* was found at temperatures below 163 °C.

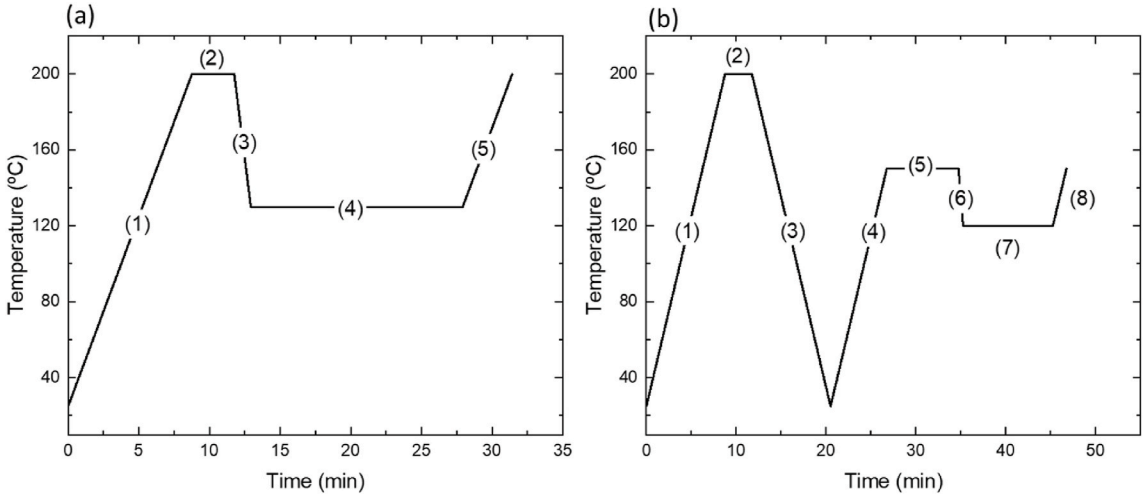

Fig. 1. Thermal protocols for studying the isothermal crystallization kinetics of (a) the polypropylene matrix phase and (b) the polyethylene-dispersed phase with crystalline PP matrix phase.

5. The material was then cooled down from T_s^{PP} to 20 °C. During this step, the effects of the thermal treatment at T_s^{PP} in the crystallization temperatures are detected.
6. Finally, a heating step was performed to know the effect of the thermal treatment on the melting temperature of the sample. *Domain II* is characterized by negligible changes in the melting endotherm compared with the ones in *Domain I*. Subsequently, a second melting peak will appear at a higher temperature due to the annealed crystals when low T_s values in *Domain III* are employed.

The protocol to study the isothermal crystallization of the PE dispersed phase (Figs. S1–b) [24] consists of the same steps numbered 1 to 4 previously described, followed by:

5. The sample was cooled from T_s^{PP} to a T_{c-iso}^{PE} temperature. The crystallization of the matrix is already completed, and depending on the T_s^{PP}, the material will be in one of the three domains.
6. The material was kept at T_{c-iso}^{PE} for different times, starting from 0 min until the accomplishment of the crystallization.
7. A final heating scan up to 225 °C displays the melting characteristics of the sample.

This last thermal protocol is denoted as isothermal step crystallization after self-nucleation of the matrix [24,35].

2.2.4. The effect of the compatibilizer on the mechanical properties

Tensile measurements were performed using an INSTRON 5569 universal testing machine at a crosshead speed of 10 mm/min according to the ASTM D638 standard. The final values are an average of five valid measurements. Izod impact resistance was measured on notched specimens using a CEAST 6548/000 pendulum according to the ASTM D256 standard. The notches (depth 2.54 mm and radius 0.25 mm) were machined after injection molding. The final values are an average of seven valid experiments.

3. Results and discussion

3.1. Morphology of the blends

Fig. 2a–c shows the characteristic sea-island morphology commonly seen in immiscible blends. In this case, PE droplets are dispersed in a PP matrix. Especially for this composition (70/30 wt%), the most thermodynamically favored morphology for the dispersed phase is the spherical one [36]. Current compatibilization strategies aim to achieve a finer morphology of blends by adding different fillers or compatibilizers. In particular, nanoparticles, copolymers, natural clays, and fillers are used for these purposes [8,11,37–39]. The addition of diblock copolymers has been studied in the literature [40] because it takes advantage of the properties of both blocks, each one able to interact specifically with one of the phases, avoiding the coalescence of the dispersed droplets, improving the interfacial adhesion between the components and therefore enhancing the final properties. Finer morphology leads to better mechanical properties due to the ease in the fracture energy dissipation process [41].

The average particle size distribution was reduced from the uncompatibilized blend (Fig. 2a) to the compatibilized ones (Fig. 2b and c). The obtained reductions for compositions 70/30/3 wt% and 70/30/6 wt% are around ~16% and ~44%, respectively (Fig. 2d). As can be seen, the average particle size shifts to a lower diameter when the amount of compatibilizer is increased. These results also indicate that a reduction in the interfacial tension between the phases occurs when the

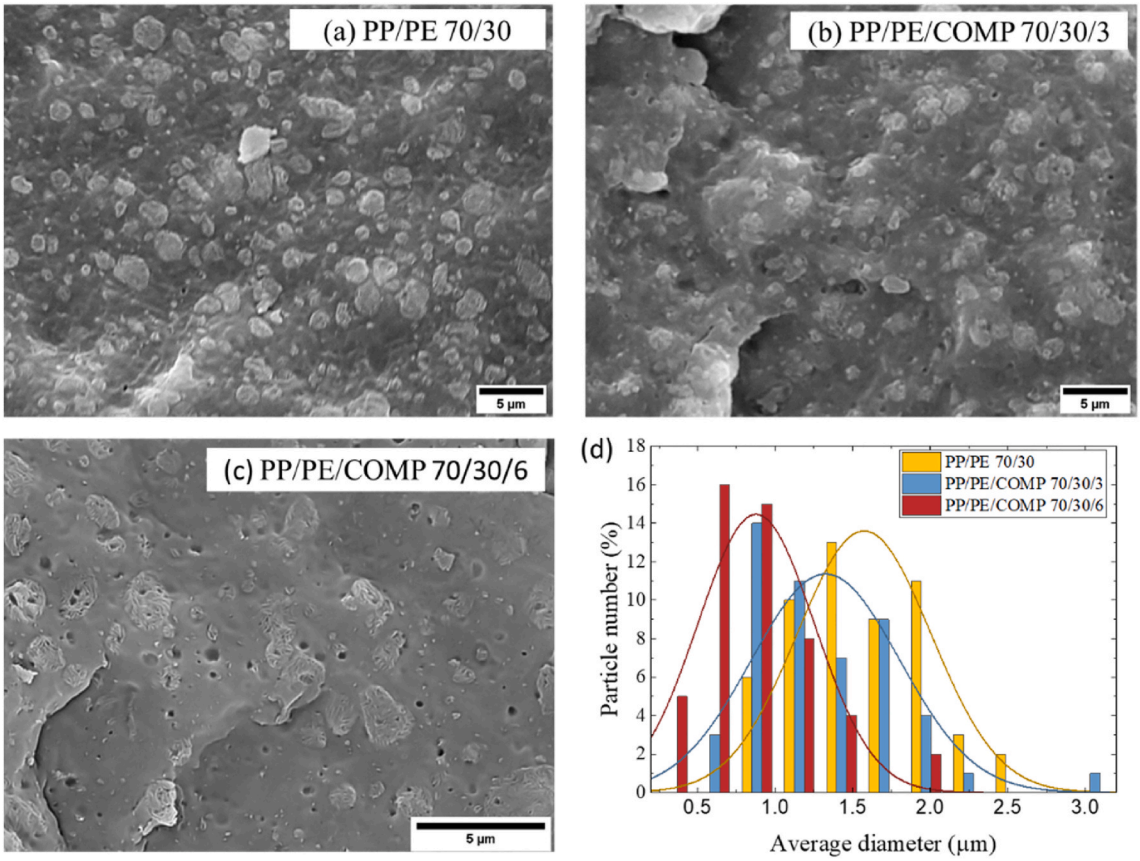

Fig. 2. Scanning electron microscopy images of (a) PP/PE (70/30), (b) PP/PE/COMP (70/30/3), (c) PP/PE/COMP (70/30/6), and (d) particle size distribution of the aforementioned blends.

compatibilizer is added.

3.2. Non-isothermal crystallization

Non-isothermal DSC cooling and heating scans, measured at a rate of 20 °C/min, are presented in Fig. 3. The separate crystallization and melting of the PP (higher temperature peak transitions) and PE (lower temperature peak transitions) phases are evident. The extracted values of the crystallization (T_c) and melting (T_m) temperatures are reported in Table 1.

During cooling, it can be observed that the measured crystallization peaks of polyethylene in the blends are moved to higher temperatures (around ~2 °C) compared to neat PE. This is because the matrix phase (PP) acts as a nucleating agent for the dispersed phase (PE). The action of the compatibilizer on the dispersed phase will also be studied via isothermal crystallization measurements (section 3.3) since a negligible effect is measured in non-isothermal conditions. On the other hand, there is no significant change in the crystallization temperature of PP in the blends with respect to the neat material.

3.3. Overall isothermal crystallization kinetics

The overall isothermal crystallization kinetics of neat PP, neat PE, and blended materials with and without compatibilizer were studied. Isothermal crystallization kinetics determined by DSC gives information about both primary nucleation and growth. The experiments were done in such a way that the isothermal kinetics of the matrix phase was measured in the presence of molten PE. Additionally, the isothermal kinetics of the PE dispersed phase were followed in the presence of a semi-crystalline PP matrix, as mentioned in the methods section (Fig. 1a).

The first parameter to be considered when studying crystallization kinetics is the incubation or induction time (t_0). Fig. 4 shows the inverse of the induction time ($1/t_0$) as a function of the crystallization temperature. The induction time corresponds to the time required to form the first stable crystalline nucleus [32,42–44]. Thus, the inverse of the induction time represents the nucleation rate. The PP/PE 70/30 and the PP/PE/COMP blends (70/30/3 and 70/30/6) show nucleation rates higher than neat PP. On the one hand, the presence of the PE dispersed phase slightly enhances the PP nucleation rate. On the other hand, a higher content of the compatibilizer results in higher nucleation rates.

Table 1
Values obtained for the thermal properties of the studied materials from DSC scans.

Sample	T_c (°C)	T_m (°C)
PP	127.4	169.4
PE	114.2	134.1
PP/PE 70/30	116.8[a]; 127.4[b]	131.4[a]; 169.2[b]
PP/PE/COMP 70/30/6	116.7[a]; 127.2[b]	132.3[a]; 169.6[b]

[a] PE.
[b] PP.

Similarly, for the isothermal crystallization measurements, in which the PP remains in its crystalline state (Fig. 4b), the nucleation rate of the dispersed PE phase increases with respect to the neat PE when blended with PP and when adding the compatibilizer. In general, the increase in the nucleation rate in both cases can be attributed to (1) a nucleating effect of the polypropylene crystals towards the dispersed PE phase and (2) an additional nucleating effect of the compatibilizer. Those results are congruent with the non-isothermal analysis previously described.

In addition, the variations in the inverse overall half crystallization time ($1/\tau_{50\%}$) are presented in Fig. 5a and b. The value of the half-crystallization time considers both nucleation and growth. For PP, an increase in the overall crystallization rate was found with the addition of the compatibilizer. A higher amount of compatibilizer increases the overall crystallization rate, even though in the non-isothermal experiments, when the sample crystallized at much higher undercooling, no changes in the crystallization temperature of PP were observable. Besides, the presence of molten PE in the PP/PE 70/30 blend does not significantly affect the overall crystallization rate, and at higher temperatures, the curve for neat PP and PP/PE 70/30 blend overlap. To corroborate this behavior, a comparison between the rate of each sample

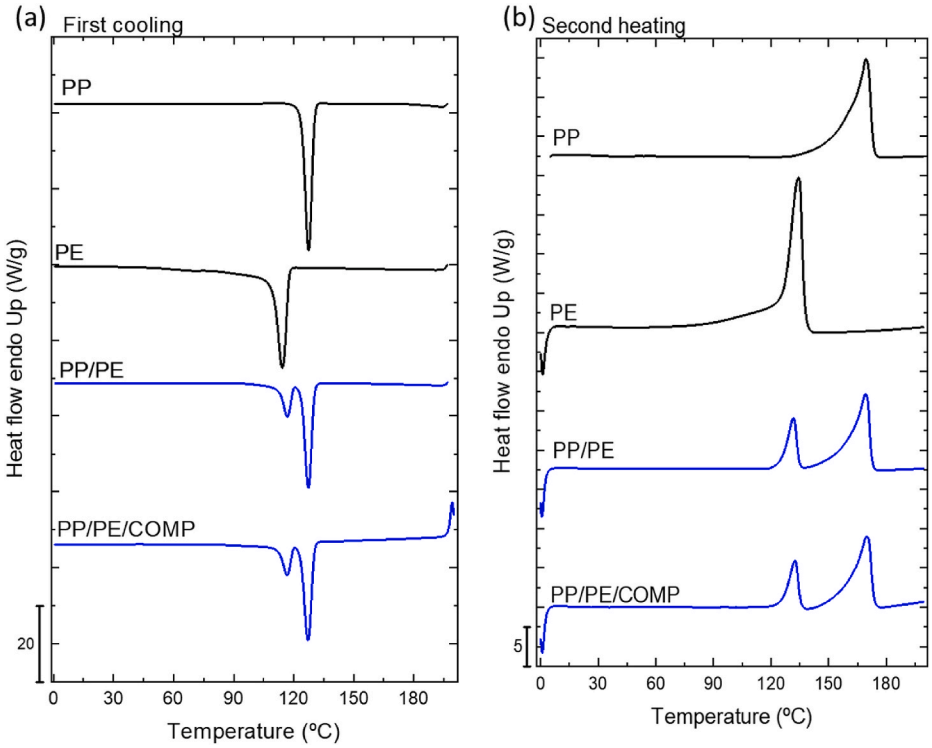

Fig. 3. (a) first DSC cooling and (b) second heating scans for neat (black curves) and blends (blue curves).

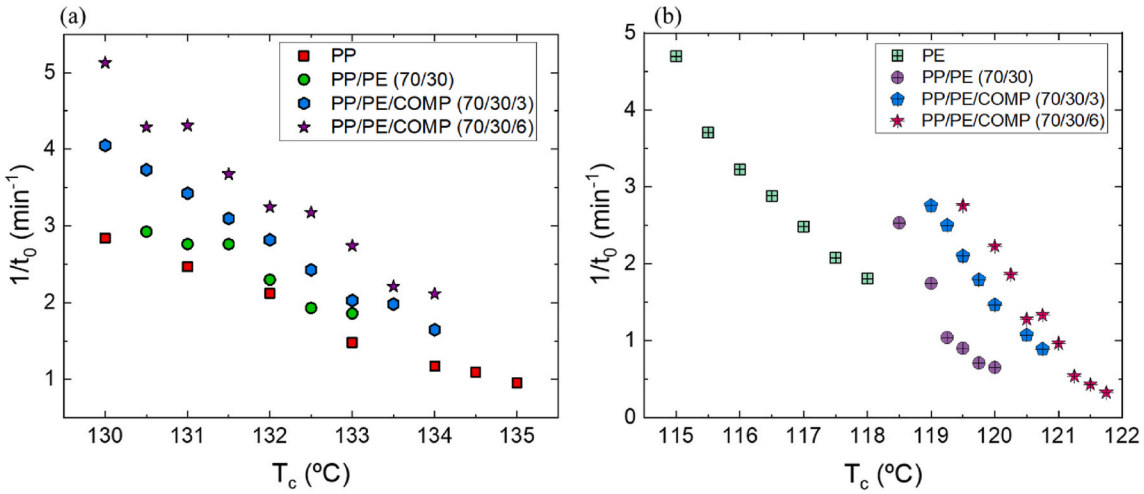

Fig. 4. Inverse of the induction time as a result of (a) isothermal crystallization of the PP phase and (b) isothermal crystallization of the dispersed phase PE within the matrix of semi-crystalline PP.

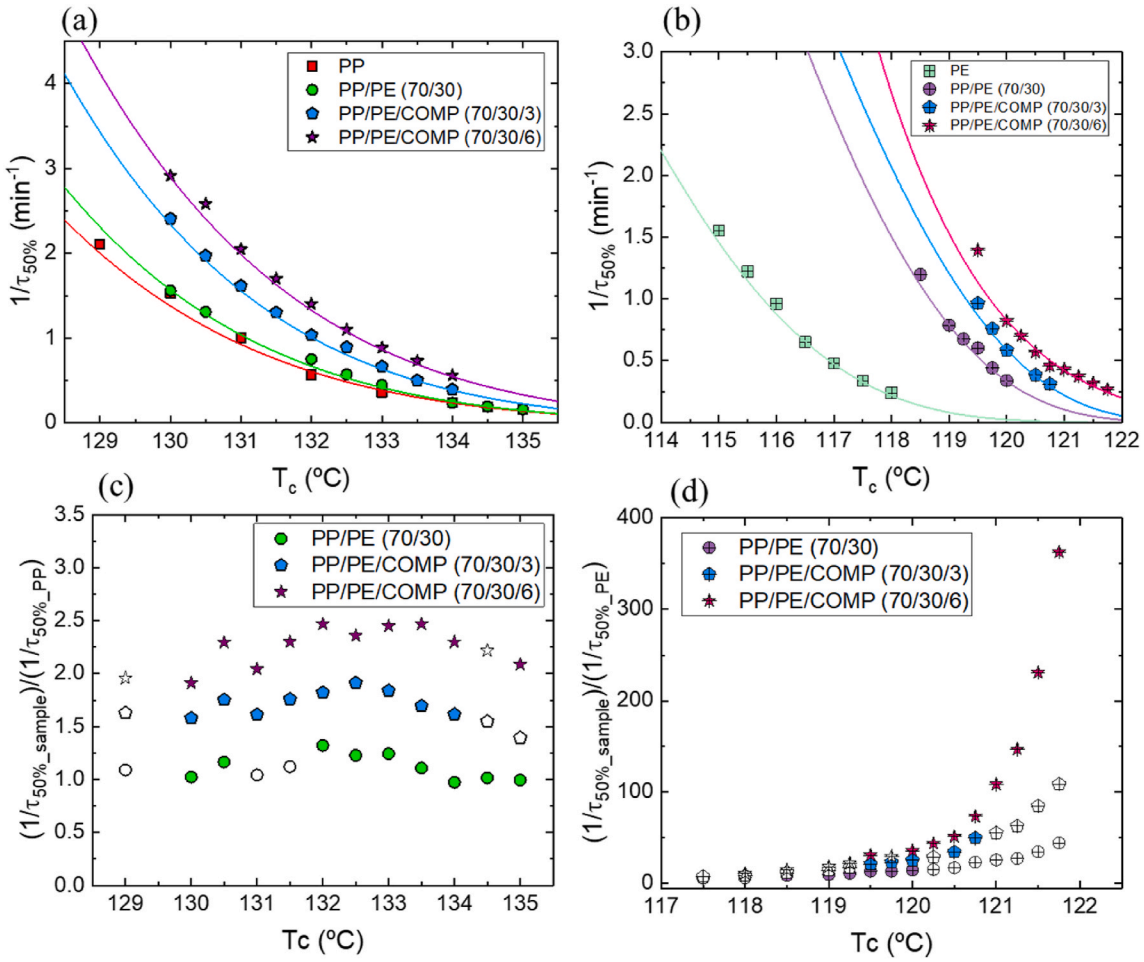

Fig. 5. Overall crystallization rate (i.e., the inverse of the experimentally determined half-crystallization time) of (a) the matrix phase (PP) and (b) the dispersed phase (PE). Solid lines correspond to the fit of the Lauritzen-Hoffman (L–H) theory. (c) Comparison between sample and neat PP and (d) comparison with neat PE. Filled points are experimental, while empty ones were obtained from the LH-fitted values.

and the rate of neat PP is presented in Fig. 5c. It is possible to see that the addition of PE in the PP/PE 70/30 curve is not affecting the crystallization rate of PP significantly as the values of the ratio $\left(\frac{1/\tau_{50\%\_sample}}{1/\tau_{50\%\_PP}}\right)$ remains almost constant. Therefore, there is no transfer of heterogeneities between phases that can promote the crystallization rate. Despite the separation of the phases due to immiscibility, the use of a compatibilizer increases the crystallization rate by a factor of 2 or more at a high concentration, which means that there is an interaction of the

compatibilizer at the interface between the phases.

On the other hand, Fig. 5b shows the overall crystallization rate of polyethylene as a dispersed phase in the presence of the crystalline PP. It is possible to observe that the overall crystallization rate increases significantly in the composition of 70/30 PP/PE. This can be explained by the presence of polypropylene crystals, which act as a nucleating surface for the dispersed polyethylene phase, increasing its overall crystallization rate. This result will be associated with the obtained mechanical properties (see Section 3.5). The presence of crystallites in the matrix phase, which act as nucleating sites, increases the intercrystalline linkage and, therefore, facilitates stress transfer, enhancing the stiffness and strengthening the material [3].

Furthermore, the addition of a compatibilizer increases the overall crystallization rate of the PE phase from 20 to almost 350 times, depending on the crystallization temperature under consideration (Fig. 5d). These results indicate a synergistic effect of the presence of PP crystals and the compatibilizer to enhance the PE droplets overall crystallization rate. In addition to the surface nucleation provided by the PP crystals at the interphase, it seems that the compatibilizer can provide additional nucleation sites, possibly by an impurity transfer effect.

The solid lines in Fig. 5 represent the fitting of the Lauritzen-Hoffman theory (L-H) to the overall crystallization rate data [45,46]. These types of compatibilizers (copolymers) can reduce interfacial tension and therefore enhance mechanical properties [40]. Furthermore, as discussed above, the crystallization rates may be enhanced with the addition of fillers and compatibilizers to polyolefin blends, and it depends on whether the interaction is chemical (reactive compatibilization) or physical (mechanical compatibilization) [6,47].

The experimental data were fitted to the Avrami equation using the free Origin© App developed by Müller et al. [32,48,49] to describe the growth of PP and PE crystals as a function of time and to obtain the respective parameters k (rate constant related to the overall crystallization kinetics) and n (Avrami index). This equation is adequate to represent the primary crystallization of polymers. For such purpose, the heat flow curve recorded during isothermal crystallization was employed to obtain the relative crystallinity (X_t) at different crystallization temperatures (T_c) as a function of crystallization time. The linearized form of the Avrami equation can be expressed in the form of [50]:

$$log[-ln(1-V_c(t-t_o))] = log\, k + n\, log(t-t_0) \quad (1)$$

where V_c stands for the relative volumetric fraction of the crystalline material, t *is* the time, and t_0 is the induction time [50]. Plotting $\log[-ln(1-V_c(t-t_o))]$ vs $\log(t-t_0)$ it is possible to obtain the slope and intercept, which are directly related to the Avrami parameters, as the slope is equal to the Avrami index and the intercept to $\log k$.

Fig. 6 shows an example of the Avrami fit obtained for the PP sample at 132 °C. The best fit of the experimental data with the Avrami equation is found at values between 3 and 25% of the conversion range, which corresponds to the primary crystallization. It is possible to observe the characteristic parameters of the fit (Avrami index, constant rate, and induction time), as well as the regression coefficient (R^2) that validates the experimental data; in this case, the value of 1 represents an excellent fit to the model. Theoretically, this model can predict the primary crystallization; however, it is anticipated to vary from the experimental data after 50% conversion because of the change from primary to secondary crystallization. This latter process is associated with the impingement of the spherulites and the crystallization that can occur in the remaining amorphous phase [50]. For all the crystallization kinetics fitted data, the regression coefficient varied from 0.998 to 1, with very small differences between the predicted and experimental data.

Fig. 7 summarizes the Avrami index for each analyzed blend. In the case of polypropylene (Fig. 7a), the Avrami index fluctuates between 2.5 and 4, which means instantaneously nucleated spherulites (values around 3) and sporadically nucleated spherulites (values around 4). Complementary, the Avrami index associated with the polyethylene

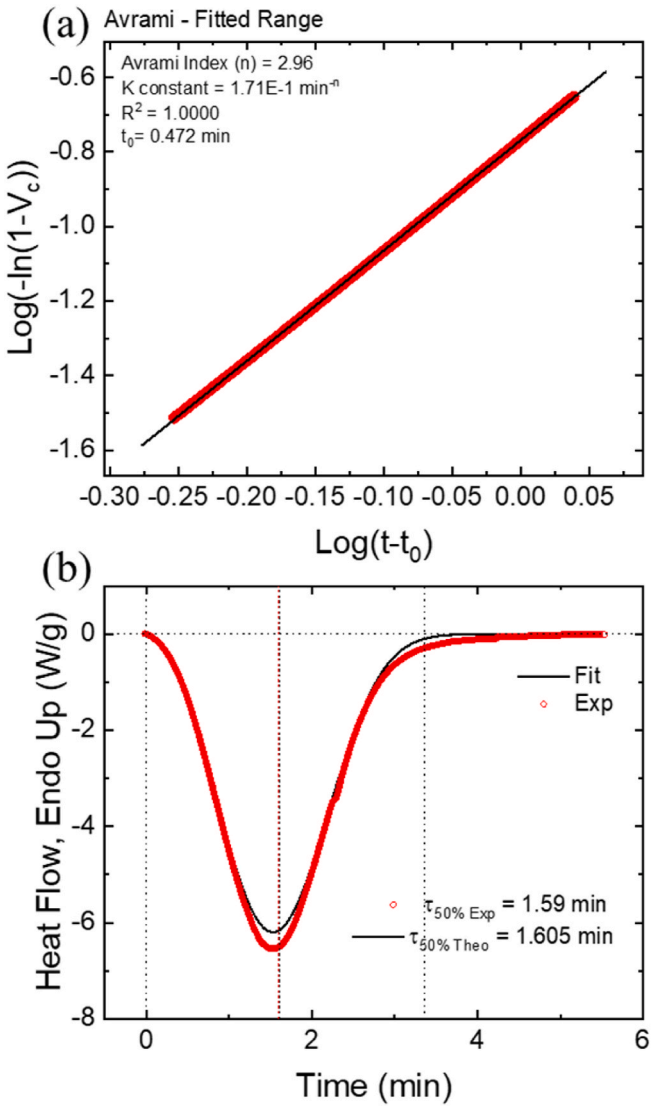

Fig. 6. Isothermal crystallization of polypropylene at 132 °C as an example of the fit: (a) Avrami plot with Vc between 3 and 25% and (b) Experimental and predicted heat flow obtained by the Avrami equation.

phase (Fig. 7b) is in the same range, except for some values at high temperatures with the use of compatibilizer, which represent instantaneously nucleated axialites rather than spherulites [51].

Another important parameter obtained through the isothermal crystallization kinetics fit at different T_c is the crystallization rate constant. Fig. 7c and d shows the change in this constant as a function of the crystallization temperature. It is worth noticing the same trends compared to the overall crystallization half-time ($1/\tau_{50\%}$), as is expected due to the excellent fitting of the Avrami equation. Note that, for a fair comparison, it was necessary to plot the constant k elevated to $1/n$ to obtain consistent units (min^{-1}). The solid lines in Fig. 7c and d represent the fit of the Lauritzen-Hoffman (L-H) theory.

As mentioned, the Lauritzen-Hoffman theory was used to fit the experimentally obtained values of the inverse of the half-time crystallization ($1/\tau_{50\%}$). The values obtained from the characteristic constants in the model (Table S1 and Table S2) are discussed in the supplementary information.

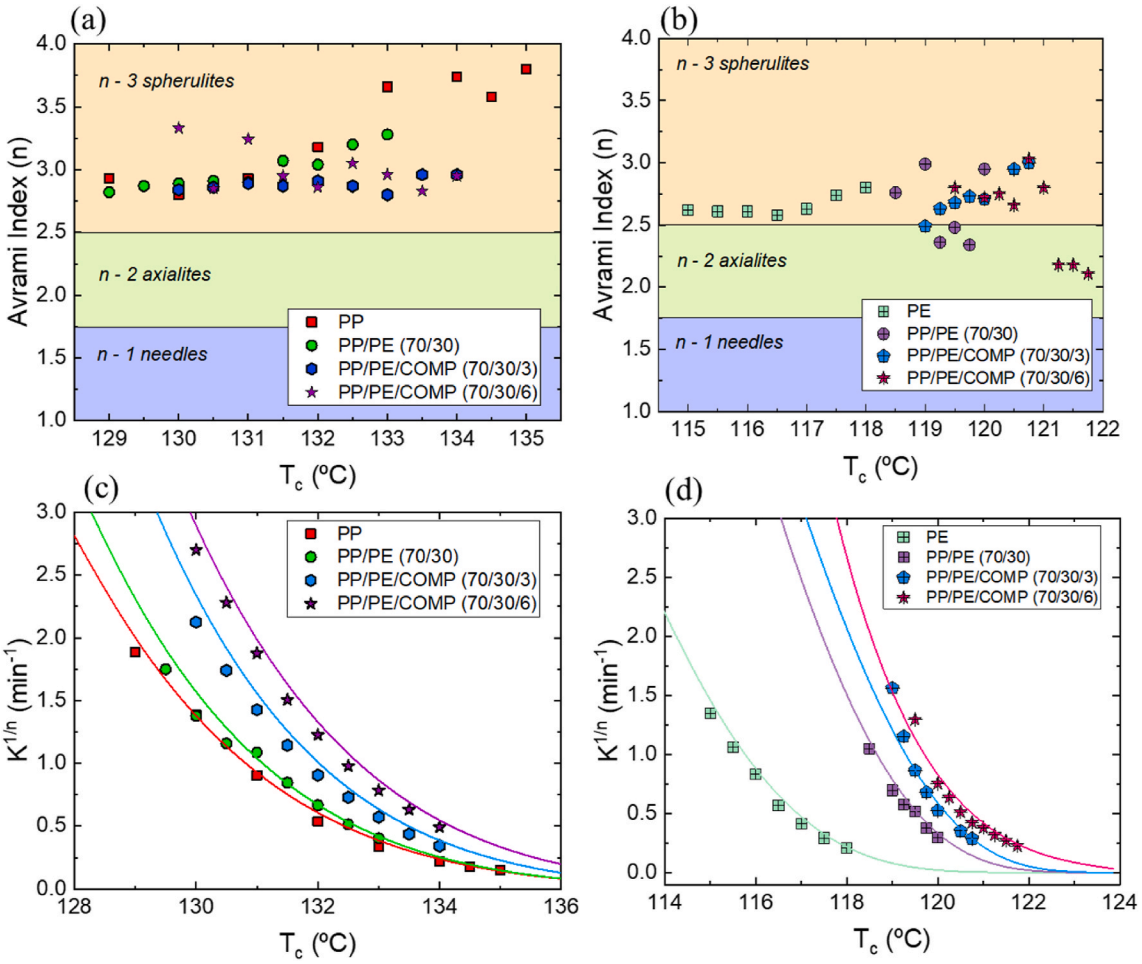

Fig. 7. Obtained values of the Avrami index in the isothermal crystallization for (a) the matrix phase (PP) and (b) the dispersed phase (PE). And crystallization constant k from the Avrami equation for (c) the matrix phase (PP) and the (d) dispersed phase (PE). Solid lines correspond to fit according to the Lauritzen-Hoffman (L–H) theory.

3.4. Self-nucleation of the matrix phase (PP) and non-isothermal crystallization of the dispersed phase (PE)

We used the self-nucleation (SN) methodology to study how it can affect the dispersed phase in the presence and absence of a compatibilizer and to compare the results with the overall isothermal kinetics shown in Section 3.3. Non-isothermal and isothermal measurements after self-nucleation of the PP matrix phase were determined.

The effect of self-nucleation on the PP matrix phase in the blends is reported in Fig. 8 for the PP/PE/COMP 70/30/3 blend. This blend was chosen as an example to show the cooling from $\boldsymbol{T_s^{PP}}$ and subsequent heating curves. The self-nucleation of a compatibilized PP/PE blend is reported here for the first time. We can readily appreciate the changes among the different self-nucleation domains. The other studied blends exhibit similar results and are reported in the supplementary information section (Fig. S2, Fig. S3), together with the definition of the three domains in neat PP (Fig. S4).

With the chosen self-nucleation temperatures (T_s), it was possible to determine all the characteristic self-nucleation domains for the matrix phase (PP) in the blend. In *Domain I*, no detectable changes in the crystallization temperature of the matrix phase were achieved, meaning that complete melting of the crystals in the matrix occurred (red curves in Fig. 8). *Domain II* was detected when the crystallization temperature (T_c) increased significantly in the cooling scans from T_s^{PP} (blue curves in Fig. 8), hence self-nucleation occurred. Therefore, a large increase in nuclei density was induced by SN, which caused an increase in the crystallization temperature [24,52]. Finally, *Domain III* was detected when an annealing peak appeared at temperatures higher than the main fusion endotherm (green curves in Fig. 8b). Note that this characteristic peak appears first at $T_s^{PP} = 164\,°C$ and is produced by the unmolten crystals that remain from the previous partial melting. This is because the unmolten crystals were annealed during the thermal treatment at T_s^{PP}. For comparison purposes, a self-nucleation protocol with the same used T_s^{PP} was performed in neat PE, see Fig. S5 and Fig. S7. The identification of the characteristic self-nucleation domains in neat PE is also shown in Fig. S6.

The T_c values for both phases across the different PP SN domains are reported in Fig. 9 as a function of the employed T_s^{PP} for all the investigated blends. In *Domain, I*, no change of T_c was found for either PP or PE phase. In addition, an increase in T_c for PE was found at T_s^{PP} in *Domain II*, which means that the higher crystallization temperature of the matrix phase facilitated the nucleation of the PE droplets at the interface. While decreasing the seeding temperature T_s^{PP}, an increment in the crystallization temperature of the PE droplets is achieved, and below a specific T_s^{PP} *Domain III* of the PP phase is reached. The total increment of the crystallization temperature for the PE dispersed phase across the SN domains of the PP phase is around 3 °C. This is a relevant result since PE is an intrinsically highly nucleated polymer and thus is difficult to increase its crystallization temperature [53].

Fig. S7 compares the changes in crystallization temperature (T_c) as a function of the seeding temperature (T_s) for neat PE and an extruded PE, as well as PE in the blended sample. For neat polyethylene, in the T_s

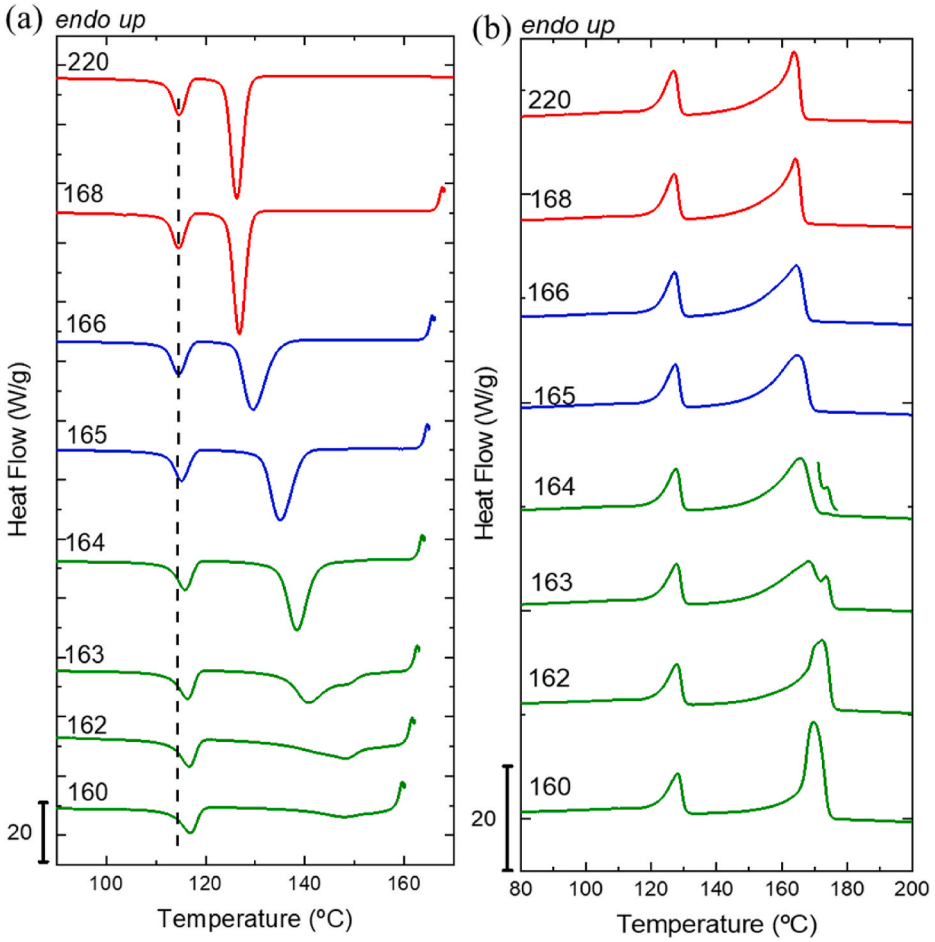

Fig. 8. DSC (a) cooling and (b) heating scans after applying the self-nucleation protocol at different T_s^{PP} temperatures for the PP/PE/COMP 70/30/3 blend. The colors in the curves are associated with the different domains: red for Domain I, blue for Domain II, and green for Domain III. In figure (b) at a T_s = 164 °C, the enlarged section of the melting trace shows the onset of the annealing peak representative of Domain III. (For interpretation of the references to color in this figure legend, the reader is referred to the Web version of this article.)

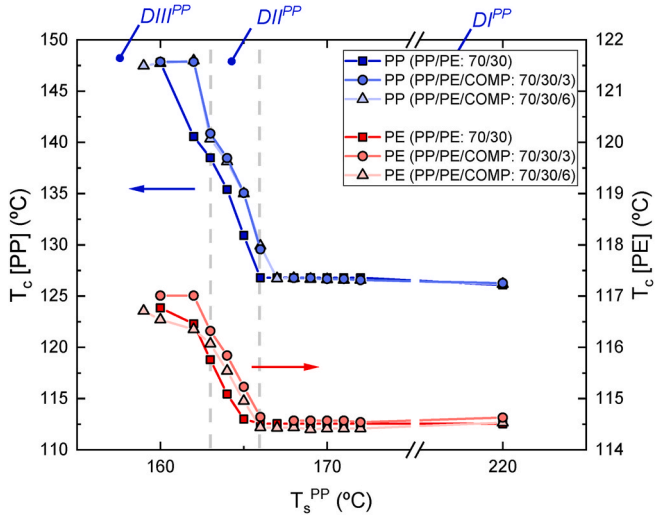

Fig. 9. T_c values for PE (right y-axis) and PP (left y-axis) in the PP/PE 70/30; PP/PE/COMP 70/30/3 and PP/PE/COMP 70/30/6 blends as a function of T_s^{PP}. The self-nucleation domains for PP and PE phases in the blend are reported.

temperature range of 127–129 °C (129 °C is the ideal self-nucleation temperature, i.e., the minimum T_s in *Domain II*, $T_{s,\ ideal}$ for neat PE), T_c increases by about 1.5 °C. At the $T_{s,\ ideal}$, the highest density of self-nuclei is achieved in the material. Remarkably, the increase in the crystallization temperature in *Domain II* of neat PE is lower than the one achieved by the blended PE at the lowest employed T_s, i.e., 160 °C. This suggests that the nucleating effect of the PP phase toward the PE phase is even larger than the nucleating effect caused by neat PE self-nuclei. As described by Fillon et al. [33], the best nucleating agents for a material should be their own self-seeds because they share the same crystal lattice and chemical structure, making the energy barrier for nucleation the lowest possible [24]. The nucleation efficiency (NE), can be calculated by the equation proposed by Fillon et al. as:

$$NE = \frac{T_c^E - T_c^{NP}}{T_c^{MNP} - T_c^{NP}} * 100 \quad (2)$$

Where T_c^E is the crystallization temperature of PE in the blends, T_c^{NP} is crystallization temperature of neat PE, and T_c^{MNP} is the maximum crystallization temperature of the ideally self-nucleated neat PE [30,54]. Therefore, the nucleation efficiency of PP to nucleate PE at the interface is presented in Table 2.

Values greater than 100% are sometimes obtained in nanocomposites (with carbon nanotubes, among other fillers), and this effect has been referred to as "*supernucleation*" [54,55]. In this case, the achievement of the *supernucleation* effect induced by the self-nucleated PP matrix phase toward the PE dispersed phase in the presence of

Table 2
Nucleation efficiency of the PP matrix on the PE dispersed phase of the indicated blends.

Sample	NE (%)
PP/PE 70/30	119 ± 17.1
PP/PE/COMP 70/30/3	124 ± 17.5
PP/PE/COMP 70/30/6	114 ± 16.6

compatibilizers is reported for the first time.

We can speculate from the results given in Table 2 that the value of nucleation efficiency increases with the addition of compatibilizer until a critical concentration is reached, and after that, it starts to decrease. This could be explained by the fact that a higher amount of compatibilizer saturates the interface between both polymers, thus affecting the aforementioned nucleation by the self-nucleated matrix PP phase and therefore decreasing the nucleation efficiency.

Isothermal crystallization of the PE phase in the presence of the self-nucleated PP matrix.

The enhancement in the crystallization temperature of the PE phase was also confirmed by the study of the isothermal crystallization kinetics of the dispersed phase. The isothermal kinetics was estimated using the melting enthalpy previously calculated from the heating steps after isothermal crystallization, as was done in a previous investigation [35].

As an example for all the materials, PP/PE/COMP 70/30/3 was chosen to represent the endotherms obtained from the heating step after the isothermal times (Fig. S8) within the protocol mentioned in Figs. S1–b. It is possible to see that the absence of the characteristic peak in the isothermal time equal to 0 min confirms the lack of crystallization during cooling from T_s^{PP} to the temperature at which isothermal crystallization was performed.

Different crystalline states of the matrix phase (PP) were employed to analyze the isothermal crystallization kinetics of the dispersed phase. Fig. 10 shows the effect of the different self-nucleation domains in the PP matrix phase on the isothermal crystallization of PE droplets. The following seeding temperatures were used across the three SN domains of PP:

- *Domain III*: $T_s^{PP} = 160°C$ and $T_s^{PP} = 163°C$
- *Domain II*: $T_s^{PP} = 165°C$
- *Domain I*: $T_s^{PP} = 200°C$

As previously discussed (see Figs. 8 and 9), the increase in the temperature (T_c) of the dispersed phase was attributed to the self-nucleation treatment in the PP matrix phase. The formation of self-nuclei in the PP as a result of the SN thermal treatment guarantees the formation of thicker PP lamellae (as PP crystallizes at higher T_c values when it is self-nucleated, and thus forms thicker lamellae, a fact corroborated in previous work by SEM and SAXS observations [24]), which can more easily nucleate the PE at the interface between both phases, resulting in the enhancement of the nucleation rate of PE. This enhancement in the crystallization rate of the PE phase was proven for different PP SN *Domains*. It is possible to see in Fig. 10 that within PP *Domain III*, the crystallization rate is the highest compared with *Domains I* and *II*. Therefore, the crystallization rate of the dispersed phase increases with the increasing dimension of the PP (matrix phase) lamellae [24].

3.4.1. Evaluation of the surface nucleation by quantitative analysis

The evaluation of the isothermal crystallization of the PE dispersed phase under the presence of the self-nucleated PP matrix phase was performed through the Avrami equation. As a saturated enthalpy value was not always reached even with large isothermal times, the obtained data were fitted with the Avrami equation in the form reported below:

$$\Delta H(t) = \Delta H_\infty \left[1 - exp\left(- (ln\ 2)\left(\frac{1}{\tau_0}(t - t_0)\right)^n\right)\right] \quad (3)$$

where ΔH_∞ is the enthalpy at saturation, τ_0 is the half-crystallization time, and t_0 is the induction time. The optimized values were the product of the fitting from the original data using a code developed in MATLAB software.

The fitting results of Eq. (3) are shown in Fig. 11 for the PP/PE/COMP 70/30/3 blend, and the obtained parameters are shown in Table 3. The optimized values for the Avrami exponent close to 1 correspond to a first-order kinetics model. The increase in crystallization temperature (T_c) results in a decrease in crystallization rate due to the larger energetic barrier associated with obtaining stable nuclei [25].

The Avrami index, half-crystallization time, enthalpy of saturation, and R^2 are reported in Table 3.

The obtained and fitted values for the PE isothermal crystallization kinetics after the self-nucleation of the PP matrix phase for the other blends are reported in the supplementary information; see Fig. S9, Fig. S10, and Fig. S11 and Table S3 and Table S4. The Avrami indexes close to 1 indicate a nucleation control in the overall crystallization kinetics of the droplets. As the temperature increases and the growth rate of the polyethylene phase decreases, the slow step of the kinetics gradually changes from nucleation control to growth control. More information is given in previous work by us [35], and in the Supplementary Information.

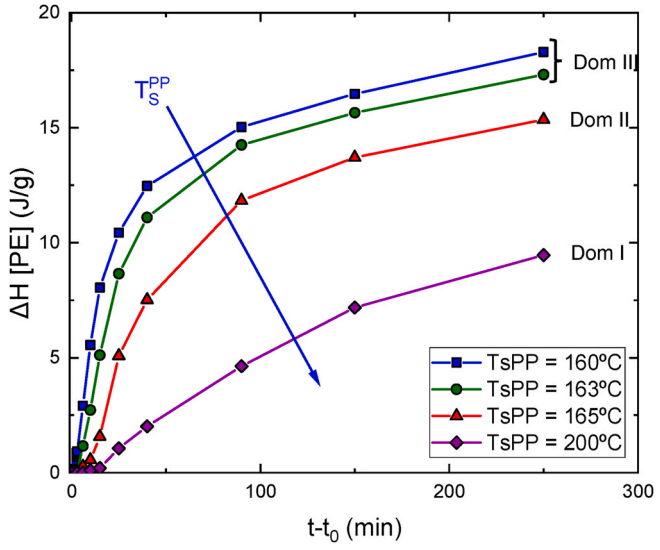

Fig. 10. Melting enthalpy of PE droplets with respect to isothermal time after the self-nucleation protocol for the matrix (PP) phase at different self-nucleation temperatures at a constant PE crystallization temperature of 123 °C for different times.

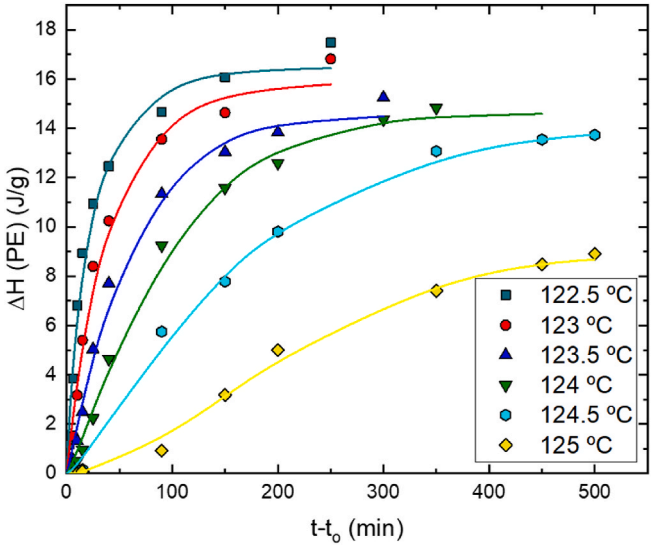

Fig. 11. Experimental (points) and fitted (lines) values of melting enthalpy for the PE phase in the PP/PE/COMP 70/30/3 blend as a function of isothermal time at different temperatures. The used T_s^{PP} was 160 °C. The lines are the result of fitting the Avrami equation.

Table 3
Crystallization parameters obtained from Fig. 11 corresponding to the PE droplets crystallizing in the PP/PE/COMP 70/30/3 blend after self-nucleation of the PP matrix at a $T_s^{PP} = 160$ °C (Domain III).

PE phase within the PP/PE/COMP 70/30/6 blend				
Temperature (°C)	Avrami index (n)	τ_c (min)	ΔH_∞ (J/g)	R^2
122.5	0.85	15.7	16.5	0.893
123	0.99	27.1	15.8	0.988
123.5	1.10	42.6	14.5	0.992
124	1.20	72.5	14.6	0.996
124.5	1.26	126.0	14.0	0.997
125	1.88	192.1	8.8	0.996

The inverse of half crystallization time ($1/\tau_{50\%}$) as a function of the isothermal time is presented in Fig. 12. It is possible to see a general tendency to decrease the value of the inverse half-crystallization time as the crystallization temperature increases. For the uncompatibilized blend, the half-crystallization time is higher in the range of crystallization temperatures of 122.5 °C to 124 °C with respect to compatibilized samples. At high temperatures, the values are equal for all three materials.

Fig. 12 shows that compatibilizer addition decreases the inverse of the half-crystallization time of the PE droplets crystallized in contact with the PP self-nucleated matrix phase. A slower crystallization rate was obtained until a specific temperature where the curves overlap. This behavior can be described by the presence of the compatibilizer at the interface between the blended polymers, which may slightly interfere with the already mentioned increased nucleating effect of the self-nucleated PP matrix phase. At higher crystallization temperatures, the inverse of the half crystallization time is very similar among the compatibilized and the uncompatibilized blends, as the nucleation probability is greatly reduced in all samples.

These results contrast with those obtained in section 3.3, where the overall isothermal kinetics were analyzed. In that section, it was shown that PP crystals and the compatibilizer provoked a synergistic increase in the overall crystallization rate of the PE phase. However, in this case, the applied SN protocol greatly enhances the number density of PP surface nucleation sites, possibly saturating the PP matrix with self-nuclei, therefore, the compatibilizer effect is unimportant. An excess of compatibilizer at the interphase can instead reduce the nucleation effect. Even though there is a slight reduction in nucleation efficiency, the self-nucleated PP matrix still exhibits a supernucleation effect even when it contains a large amount of compatibilizer at the interphase.

Crystallinity values were also obtained to analyze the isothermal crystallization of the PE dispersed phase, as shown in Fig. 13. In general, the value of PE crystallinity is higher for the uncompatibilized blend except at 124.5 °C. The trend shows a reduction in the crystallinity as the crystallization temperature increases. It is worth pointing out the similarity of the results for compatibilized blends with different amounts of compatibilizer. These results agree with the PE overall crystallization kinetics presented in Fig. 12. Since the PE droplets in the blends with compatibilizer have a slower crystallization rate in the low T_c range, they also form a lower amount of PE crystals in comparison with the uncompatibilized blend. In addition, the obtained crystallization and melting enthalpy values for both phases (PP and PE) in the blends as a function of the T_s^{PP} is presented in the supplementary information (Fig. S12).

3.5. Mechanical properties of the compatibilized blends

Stress-strain tests were performed to evaluate the tensile mechanical behavior of neat PP and PE and blended compositions (PP/PE 70/30, PP/PE/COMP 70/30/3, and PP/PE/COMP 70/30/6). Fig. 14 shows representative curves of the studied materials. As it can be seen, except for neat PE that failed during necking, neat PP and blends presented the characteristic stress-strain curves of ductile materials, showing a broad yielding peak corresponding to the necking process, followed by an extensive plateau in the stress corresponding to neck propagation [56] and a final stress increase related to the strain-hardening process.

Fig. 14 shows Young modulus and ductility values for all the compositions studied. As can be seen, Young moduli of the uncompatibilized blends follow the additivity rule, as usual in immiscible polymer blends [3,57]. When compared to those of compatibilized compositions, small differences, close to the experimental error of the measurement, were observed, with a slight increase at lower compatibilizer content and a further decrease at the highest compatibilizer content, indicating that the effect of the compatibilization on Young modulus, if any, reaches a maximum at an optimum compatibilizer concentration. This is not an unusual result, as has also been observed in other compatibilized blends [3,39,58,59].

Regarding ductility, and as shown in Fig. 15, the uncompatibilized PP/PE blend showed a high deformation at break value (close to 300%), even higher than neat PP. This is a surprising and favorable behavior in

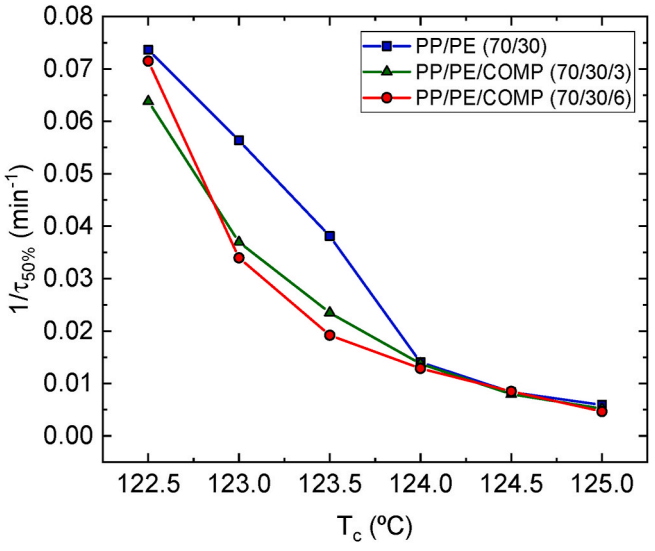

Fig. 12. The inverse of the crystallization half-time for PE droplets obtained from the fitting of Eq. (3) as a function of the crystallization temperature (T_c).

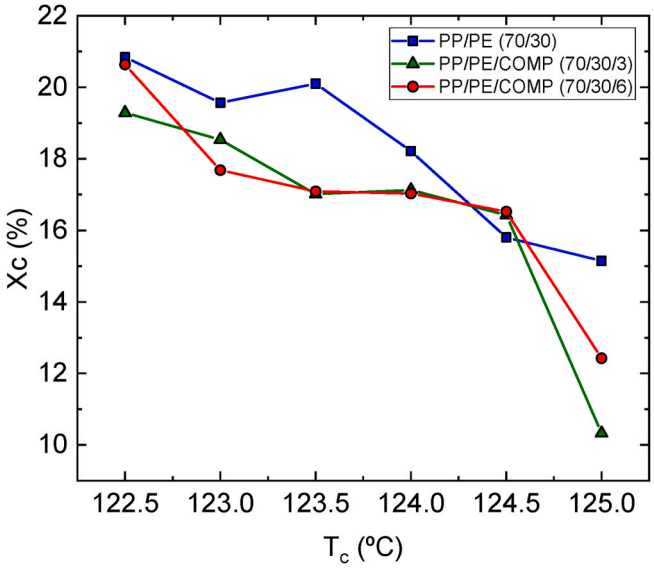

Fig. 13. Crystallinity of the polyethylene droplets in the blends as a function of the isothermal crystallization temperature.

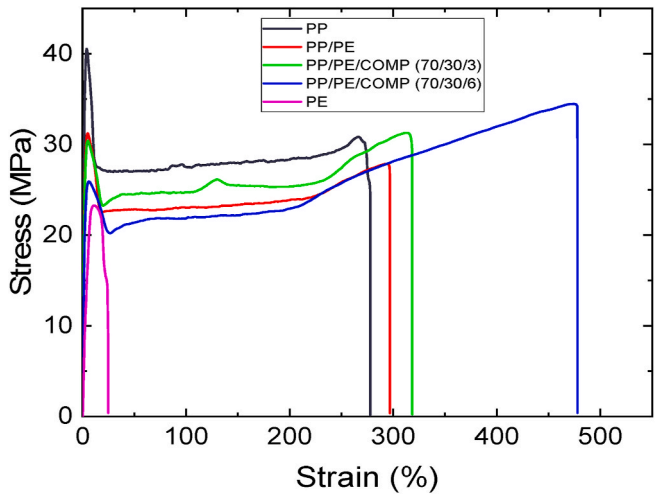

Fig. 14. Stress-strain curves of the neat and blended materials.

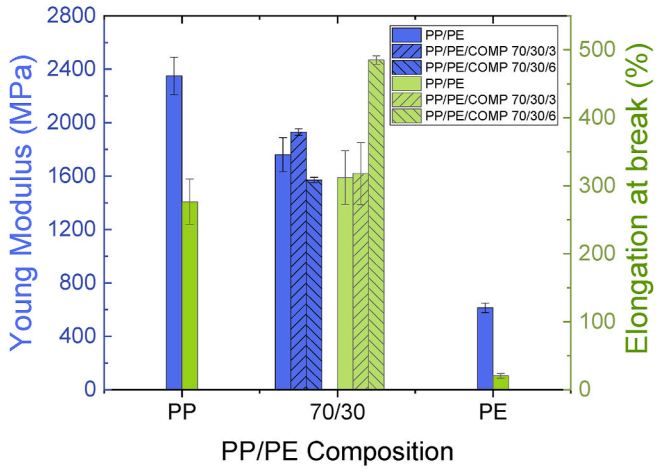

Fig. 15. Young modulus (blue columns) and elongation at break (green columns) values of neat and blended materials. (For interpretation of the references to color in this figure legend, the reader is referred to the Web version of this article.)

an immiscible blend because these blends usually show ductility values well below the additivity rule between pure components, owing to large particle sizes and low interfacial adhesion between the matrix and dispersed phase [7]. However, similar results have been obtained for PP/LDPE systems [60], and they were attributed to the type of interface arrangement between both polymers and the morphological characteristics [56,60]. Concerning compatibilized blends, they showed a slight increase in ductility at the lower compatibilizer content (70/30/3) and a very significant increase at the maximum content (close to 500% elongation at break value for composition 70/30/6). Using an effective compatibilizer in PP/PE blends is expected to enhance the ductility of the blends without significantly affecting strength and stiffness [3] due to a reduction of the interfacial tension between phases, thus obtaining a finer morphology [3,39,58,59]. This leads to better mechanical properties because it favors stress transfer between phases and thus prevents early crack initiation at the interface [41,61]. In our case, a higher compatibilizer content (70/30/6) leads to an improvement of around ~40% in ductility compared to the uncompatibilized blend. The obtained value is considerably higher than in the neat polymers, representing a great advantage for specific applications, such as packaging [62].

Impact resistance is also essential in defining the mechanical characteristics of polymeric materials. Table 4 shows the Izod impact resistance values obtained for the neat PP and blended materials. As can be seen, the impact resistance is significantly higher (~100%) in the blends than in the neat PP due to the presence of the dispersed PE. Similar results have been obtained in polypropylene-copolymer blended with high-density polyethylene systems, where the increase in toughness was attributed to the addition of HDPE [63]. Concerning the effect of the addition of the compatibilizer, although slightly higher in the compatibilized blends than in the case of the uncompatibilized one, the differences are close to the experimental error of the measurement, and the values obtained for the blends with different compatibilizer contents are similar.

The impact resistance is associated with the capability of a material to resist an applied load at high deformation speed [64], which is very important in high-demand resistance applications such as automotive industries. Blending commodity materials such as PP and PE leads the way to further applying the same strategies in recycled streams.

4. Conclusions

The effect of adding a commercial ethylene-*ran*-methyl acrylate random copolymer on the morphology, crystallization, and mechanical properties of PP/PE blends has been investigated. Novel results about the effect of the compatibilizer on the crystallization kinetics were found. A nucleating effect of the polypropylene matrix phase towards the polyethylene dispersed phase was obtained, further synergistically enhanced by compatibilizer addition.

Furthermore, it was observed that applying a self-nucleation (SN) thermal treatment to the PP matrix phase provoked changes in the crystallinity of the PE dispersed phase and its crystallization rate. An increment in the crystallization temperature of the polyethylene phase was obtained because of the presence of a self-nucleated PP matrix. The obtained nucleation efficiency was >114% for all blends obtaining a *supernucleating* effect. However, when a higher amount of compatibilizer was added, the nucleation efficiency was decreased. This result was explained considering that the amount of compatibilizer was high enough to saturate the interface between both polymers, thus reducing the nucleation effect of the self-nucleated PP matrix. In agreement, the overall crystallization rate of the PE phase under the presence of a self-nucleated PP matrix phase and compatibilizer decreased with respect to the uncompatibilized blend, corroborating the decrease in the nucleation efficiency.

Finally, The use of the compatibilizer in the 70/30/6 blend increased the ductility by around ~40%. The morphological analysis agrees with the mechanical and thermal analysis in that a reduction of about ~44% was observed in the average particle size.

Funding

All of the sources of funding for the work described in this publication are acknowledged below:

This work has received funding from the European Union's Horizon 2020 research and innovation program under Grant Agreement No 860221 under the name of the REPOL project.

Table 4
Obtained values for Izod impact resistance measurements.

Sample	Impact resistance (J/m)
PP	14.5 ± 1.2
PP/PE (70/30)	28.6 ± 4.2
PP/PE/COMP (70/30/3)	30.8 ± 1.2
PP/PE/COMP (70/30/6)	31.7 ± 3.4

Declaration of competing interest

The authors declare that they have no known competing financial interests or personal relationships that could have appeared to influence the work reported in this paper.

Data availability

Data will be made available on request.

Acknowledgements

We acknowledge the financial support from the REPOL project; this project has received funding from the European Union's Horizon 2020 research and innovation program under the Marie Skłodowska-Curie Grant Agreement No. 860221. The authors thank Diana Sánchez for her support in performing some DSC measurements.

Appendix A. Supplementary data

Supplementary data to this article can be found online at https://doi.org/10.1016/j.polymer.2022.125511.

References

[1] M.N. Subramanian, Chapter 5: polymer blends and composites, in: Polym. Blends Compos., John Wiley & Sons, Inc., 2017, pp. 113–151, https://doi.org/10.1002/9781119383581.
[2] S. Kumar, A.K. Panda, R.K. Singh, A review on tertiary recycling of high-density polyethylene to fuel, Resour. Conserv. Recycl. 55 (2011) 893–910, https://doi.org/10.1016/J.RESCONREC.2011.05.005.
[3] A. Graziano, S. Jaffer, M. Sain, Review on modification strategies of polyethylene/polypropylene immiscible thermoplastic polymer blends for enhancing their mechanical behavior, J. Elastomers Plastics 51 (2019) 291–336, https://doi.org/10.1177/0095244318783806.
[4] S. Vervoort, J. den Doelder, E. Tocha, J. Genoyer, K.L. Walton, Y. Hu, J. Munro, K. Jeltsch, Compatibilization of polypropylene–polyethylene blends, Polym. Eng. Sci. 58 (2018) 460–465, https://doi.org/10.1002/PEN.24661.
[5] C. Tselios, D. Bikiaris, V. Maslis, C. Panayiotou, In situ compatibilization of polypropylene–polyethylene blends: a thermomechanical and spectroscopic study, Polymer (Guildf) 39 (1998) 6807–6817, https://doi.org/10.1016/S0032-3861(98)00132-3.
[6] T. Kallel, V. Massardier-Nageotte, M. Jaziri, J.-F.F. Gérard, B. Elleuch, Compatibilization of PE/PS and PE/PP blends. I. Effect of processing conditions and formulation, J. Appl. Polym. Sci. 90 (2003) 2475–2484, https://doi.org/10.1002/app.12873.
[7] L.A. Utracki, Compatibilization of polymer blends, Can. J. Chem. Eng. 80 (2002) 1008–1016, https://doi.org/10.1002/CJCE.5450800601.
[8] A. Taguet, P. Cassagnau, J.M. Lopez-Cuesta, Structuration, selective dispersion and compatibilizing effect of (nano)fillers in polymer blends, Prog. Polym. Sci. 39 (2014) 1526–1563.
[9] X. Jing, Y. Li, J. Zhu, L. Chang, S. Maganti, N. Naik, B. Bin Xu, V. Murugadoss, M. Huang, Z. Guo, Improving thermal conductivity of polyethylene/polypropylene by styrene-ethylene-propylene-styrene wrapping hexagonal boron nitride at the phase interface, Adv. Compos. Hybrid. Mater. 5 (2022) 1090–1099, https://doi.org/10.1007/S42114-022-00438-X/FIGURES/5.
[10] I. Fortelný, Z. Kruliš, D. Michálková, Z. Horák, Effect of EPDM admixture and mixing conditions on the morphology and mechanical properties of LDPE/PP blends, Angew. Makromol. Chem. 238 (1996) 97–104, https://doi.org/10.1002/APMC.1996.052380109.
[11] B. Su, Y.G. Zhou, H.H. Wu, Influence of mechanical properties of polypropylene/low-density polyethylene nanocomposites: compatibility and crystallization, Nanomater. Nanotechnol. 7 (2017), 184798041771592, https://doi.org/10.1177/1847980417715929.
[12] A. Graziano, S. Jaffer, M. Sain, Review on modification strategies of polyethylene/polypropylene immiscible thermoplastic polymer blends for enhancing their mechanical behavior, J. Elastomers Plastics 51 (2019) 291–336, https://doi.org/10.1177/0095244318783806/ASSET/IMAGES/LARGE/10.1177_0095244318783806-FIG2.JPEG.
[13] K. Klimovica, S. Pan, T.W. Lin, X. Peng, C.J. Ellison, A.M. Lapointe, F.S. Bates, G. W. Coates, Compatibilization of iPP/HDPE blends with PE-g-iPP graft copolymers, ACS Macro Lett. 9 (2020) 1161–1166, https://doi.org/10.1021/acsmacrolett.0c00339.
[14] N.D. Tien, R.E. Prud'homme, Crystallization behavior of semicrystalline immiscible polymer blends, Cryst. Multiphas. Polym. Syst. (2018) 181–212, https://doi.org/10.1016/B978-0-12-809453-2.00007-4.
[15] R. Scaffaro, F.P. La Mantia, L. Canfora, G. Polacco, S. Filippi, P. Magagnini, Reactive compatibilization of PA6/LDPE blends with an ethylene–acrylic acid copolymer and a low molar mass bis-oxazoline, Polymer (Guildf) 44 (2003) 6951–6957, https://doi.org/10.1016/J.POLYMER.2003.06.001.
[16] F. Rybnikář, Http://Dx.Doi.Org/10.1080/00222348808245759, Crystallization and Morphology in Blends of Isotactic Polypropylene and Linear Polyethylene, vol. 27, 2006, pp. 125–144, https://doi.org/10.1080/00222348808245759.
[17] C.W. Macosko, H.K. Jeon, T.R. Hoye, Reactions at polymer–polymer interfaces for blend compatibilization, Prog. Polym. Sci. 30 (2005) 939–947, https://doi.org/10.1016/J.PROGPOLYMSCI.2005.06.003.
[18] J. Zhang, P.J. Cole, U. Nagpal, C.W. Macosko, T.P. Lodge, Https://Doi.Org/10.1080/00218460600875847, Direct Correlation between Adhesion Promotion and Coupling Reaction at Immiscible Polymer-Polymer Interfaces, vol. 82, 2006, pp. 887–902, https://doi.org/10.1080/00218460600875847.
[19] N. Aranburu, J.I. Eguiazabal, Compatible blends of polypropylene with an amorphous polyamide, J. Appl. Polym. Sci. 127 (2013) 5007–5013, https://doi.org/10.1002/APP.38090.
[20] N. Aranburu, J.I. Eguiazábal, Improved mechanical properties of compatibilized polypropylene/polyamide-12 blends, 2015, Int. J. Polym. Sci. (2015), https://doi.org/10.1155/2015/742540.
[21] R.T. Tol, V.B.F. Mathot, G. Groeninckx, Confined crystallization phenomena in immiscible polymer blends with dispersed micro- and nanometer sized PA6 droplets, part 2: reactively compatibilized PS/PA6 and (PPE/PS)/PA6 blends, Polymer (Guildf) 46 (2005) 383–396, https://doi.org/10.1016/J.POLYMER.2004.10.070.
[22] Q. Wei, D. Chionna, E. Galoppini, M. Pracella, Functionalization of LDPE by melt grafting with glycidyl methacrylate and reactive blending with polyamide-6, Macromol. Chem. Phys. 204 (2003) 1123–1133, https://doi.org/10.1002/macp.200390081.
[23] C. Yordanov, L. Minkova, Fractionated crystallization of compatibilized LDPE/PA6 blends, Eur. Polym. J. 41 (2005) 527–534, https://doi.org/10.1016/J.EURPOLYMJ.2004.10.034.
[24] E. Carmeli, S.E. Fenni, M.R. Caputo, A.J. Müller, D. Tranchida, D. Cavallo, Surface nucleation of dispersed polyethylene droplets in immiscible blends revealed by polypropylene matrix self-nucleation, Macromolecules 54 (2021) 9100–9112, https://doi.org/10.1021/acs.macromol.1c01430.
[25] B. Wunderlich, The nucleation step, in: Macromol. Phys., Academic Press, 1976, https://doi.org/10.1016/b978-0-12-765602-1.50007-0, 1–114.
[26] J. Ibarretxe, G. Groeninckx, L. Bremer, V.B.F. Mathot, Quantitative evaluation of fractionated and homogeneous nucleation of polydisperse distributions of water-dispersed maleic anhydride-grafted-polypropylene micro- and nano-sized droplets, Polymer (Guildf) 50 (2009) 4584–4595, https://doi.org/10.1016/J.POLYMER.2009.06.067.
[27] M.L. Arnal, A.J. Müller, Fractionated crystallisation of polyethylene and ethylene/α-olefin copolymers dispersed in immiscible polystyrene matrices, Macromol. Chem. Phys. 200 (1999) 2559–2576, https://doi.org/10.1002/(SICI)1521-3935(19991101)200:11<2559::AID-MACP2559>3.0.CO;2-O.
[28] M.L. Arnal, A.J. Müller, P. Maiti, M. Hikosaka, Nucleation and crystallization of isotactic poly(propylene) droplets in an immiscible polystyrene matrix, Macromol. Chem. Phys. 201 (2000) 2493–2504, https://doi.org/10.1002/1521-3935.
[29] L. Sangroniz, B. Wang, Y. Su, G. Liu, D. Cavallo, D. Wang, A.J. Müller, Fractionated crystallization in semicrystalline polymers, Prog. Polym. Sci. 115 (2021), 101376, https://doi.org/10.1016/J.PROGPOLYMSCI.2021.101376.
[30] R.M. Michell, A. Mugica, M. Zubitur, A.J. Muller, Self-nucleation of crystalline phases within homopolymers, polymer blends, copolymers, and nanocomposites, Adv. Polym. Sci. 276 (2015) 215–256, https://doi.org/10.1007/12_2015_327.
[31] M. Aboulfaraj, B. Ulrich, A. Dahoun, C. G'Sell, Spherulitic morphology of isotactic polypropylene investigated by scanning electron microscopy, Polymer (Guildf) 34 (1993) 4817–4825, https://doi.org/10.1016/0032-3861(93)90003-S.
[32] A.T. Lorenzo, M.L. Arnal, J. Albuerne, A.J. Müller, DSC isothermal polymer crystallization kinetics measurements and the use of the Avrami equation to fit the data: guidelines to avoid common problems, Polym. Test. 26 (2007) 222–231, https://doi.org/10.1016/J.POLYMERTESTING.2006.10.005.
[33] B. Fillon, J.C. Wittmann, B. Lotz, A. Thierry, Self-nucleation and recrystallization of isotactic polypropylene (α phase) investigated by differential scanning calorimetry, J. Polym. Sci., Part B: Polym. Phys. 31 (1993) 1383–1393, https://doi.org/10.1002/POLB.1993.090311013.
[34] L. Sangroniz, D. Cavallo, A.J. Müller, Self-nucleation effects on polymer crystallization, Macromolecules 53 (2020) 4581–4604, https://doi.org/10.1021/ACS.MACROMOL.0C00223/ASSET/IMAGES/LARGE/MA0C00223_0003.JPEG.
[35] B. Wang, R. Utzeri, M. Castellano, P. Stagnaro, A.J. Müller, D. Cavallo, Heterogeneous nucleation and self-nucleation of isotactic polypropylene microdroplets in immiscible blends: from nucleation to growth-dominated crystallization, Macromolecules 53 (2020) 5980–5991, https://doi.org/10.1021/acs.macromol.0c01167.
[36] Z. Starý, Thermodynamics and morphology and compatibilization of polymer blends, in: Charact. Polym. Blends Miscibility, Morphol. Interfaces, John Wiley & Sons, Ltd, 2015, pp. 93–132, https://doi.org/10.1002/9783527645602.CH03.
[37] A.C. Baudouin, D. Auhl, F. Tao, J. Devaux, C. Bailly, Polymer blend emulsion stabilization using carbon nanotubes interfacial confinement, Polymer (Guildf) 52 (2011) 149–156, https://doi.org/10.1016/J.POLYMER.2010.11.004.
[38] J. Xu, J.M. Eagan, S.-S. Kim, S. Pan, B. Lee, K. Klimovica, K. Jin, T.-W. Lin, M. J. Howard, C.J. Ellison, A.M. LaPointe, G.W. Coates, F.S. Bates, Compatibilization of isotactic polypropylene (iPP) and high-density polyethylene (HDPE) with iPP–PE multiblock copolymers, Macromolecules 51 (2018) 8585–8596, https://doi.org/10.1021/ACS.MACROMOL.8B01907.
[39] M.A.H. Ibrahim, A. Hassan, M.U. Wahit, M. Hasan, M. Mokhtar, Mechanical properties and morphology of polypropylene/poly

(acrylonitrile–butadiene–styrene) nanocomposites, J. Elastomers Plastics 49 (2017) 209–225, https://doi.org/10.1177/0095244316644859.
[40] I. Fortelný, J. Jůza, The effects of copolymer compatibilizers on the phase structure evolution in polymer blends—a review, 14 (2021) 7786, Mater 14 (2021) 7786, https://doi.org/10.3390/MA14247786.
[41] H. Liu, T. Xie, Y. Zhang, O.U. Yuchun, G. Yang, Phase morphology development in PP/PA6 blends induced by a maleated thermoplastic elastomer, J. Polym. Sci., Part B: Polym. Phys. 44 (2006) 1050–1061, https://doi.org/10.1002/POLB.20765.
[42] F.J. Baltá-Calleja, T.A. Ezquerra, Polymer crystallization: general concepts of theory and experiments, in: Encycl. Mater. Sci. Technol., Elsevier, 2001, pp. 7244–7252, https://doi.org/10.1016/b0-08-043152-6/01289-4.
[43] M. Imai, K. Mori, T. Mizukami, K. Kaji, T. Kanaya, Structural formation of poly (ethylene terephthalate) during the induction period of crystallization: 2. Kinetic analysis based on the theories of phase separation, Polymer (Guildf). 33 (1992) 4457–4462, https://doi.org/10.1016/0032-3861(92)90400-Q.
[44] M. Eesaee, A.J. Müller, P. O'Reilly, R.E. Prud'homme, P. Nguyen-Tri, Miscibility, morphology, and crystallization kinetics of biodegradable poly(ε-caprolactone)/ascorbic acid blends, ACS Appl. Polym. Mater. 4 (2022) 301–312, https://doi.org/10.1021/acsapm.1c01307.
[45] J.D. Hoffman, J.I. Lauritzen Jr., Crystallization of bulk polymers with chain folding: theory of growth of lamellar spherulites, J. Res. Natl. Bur. Stand. Sect. A, Phys. Chem. 65A (1961) 297, https://doi.org/10.6028/JRES.065A.035.
[46] A.T. Lorenzo, A.J. Müller, Estimation of the nucleation and crystal growth contributions to the overall crystallization energy barrier, J. Polym. Sci., Part B: Polym. Phys. 46 (2008) 1478–1487, https://doi.org/10.1002/POLB.21483.
[47] J. Girones, L.T.T. Vo, J.M. Haudin, L. Freire, P. Navard, Crystallization of polypropylene in the presence of biomass-based fillers of different compositions, Polymer (Guildf) 127 (2017) 220–231, https://doi.org/10.1016/J.POLYMER.2017.09.006.
[48] Origin Lab, Crystallization Fit , (n.d.). https://www.originlab.com/fileExchange/details.aspx?fid=597 (accessed February 15, 2022).
[49] R.A. Pérez-Camargo, G.M. Liu, D.J. Wang, A.J. Müller, Experimental and data fitting guidelines for the determination of polymer crystallization kinetics, Chinese J. Polym. Sci. (English Ed. 40 (2022) 658–691, https://doi.org/10.1007/s10118-022-2724-2.
[50] A.J. Müller, R.M. Michell, A.T. Lorenzo, Isothermal crystallization kinetics of polymers, Polym. Morphol. Princ. Charact. Process. (2016) 181–203, https://doi.org/10.1002/9781118892756.CH11.
[51] E. Schulz, B. Wunderlich, Macromolecular physics, vol. 2 crystal nucleation, growth, annealing, Krist. Tech. 12 (1977) K11–K12, https://doi.org/10.1002/CRAT.19770120121.
[52] J. Wagner, P.J. Phillips, The mechanism of crystallization of linear polyethylene, and its copolymers with octene, over a wide range of supercoolings, Polymer (Guildf) 42 (2001) 8999–9013, https://doi.org/10.1016/S0032-3861(01)00386-X.
[53] H. Jiang, X. Zhang, J. Qiao, Different influences of nucleating agents on crystallization behavior of polyethylene and polypropylene, 2012, Sci. China Chem. 556 (55) (2012) 1140–1147, https://doi.org/10.1007/S11426-012-4516-Y.
[54] M. Trujillo, M.L. Arnal, A.J. Müller, M.A. Mujica, C. Urbina De Navarro, B. Ruelle, P. Dubois, Supernucleation and crystallization regime change provoked by MWNT addition to poly(ε-caprolactone), Polymer (Guildf) 53 (2012) 832–841, https://doi.org/10.1016/J.POLYMER.2011.12.028.
[55] A.J. Müller, M.L. Arnal, M. Trujillo, A.T. Lorenzo, Super-nucleation in nanocomposites and confinement effects on the crystallizable components within block copolymers, miktoarm star copolymers and nanocomposites, in: Eur. Polym. J., Pergamon, 2011, pp. 614–629, https://doi.org/10.1016/j.eurpolymj.2010.09.027.
[56] C.M. Tai, R.K.Y. Li, C.N. Ng, Impact behaviour of polypropylene/polyethylene blends, Polym. Test. 19 (2000) 143–154, https://doi.org/10.1016/S0142-9418(98)00080-4.
[57] J. Parameswaranpillai, G. Joseph, S. Jose, N. Hameed, Phase morphology, thermomechanical, and crystallization behavior of uncompatibilized and PP-g-MAH compatibilized polypropylene/polystyrene blends, J. Appl. Polym. Sci. 132 (2015), 42100, https://doi.org/10.1002/APP.42100.
[58] J. Parameswaranpillai, S. Thomas, Y. Grohens, Polymer blends: state of the art, new challenges, and opportunities, charact. Polym. Blends miscibility, Morphol. Interfaces. 9783527331536 (2015) 1–6, https://doi.org/10.1002/9783527645602.CH01.
[59] E.M. Akshaya, R. Palaniappan, C.F. Sowmya, N. Rasana, K. Jayanarayanan, Properties of blends from polypropylene and recycled polyethylene terephthalate using a compatibilizer, Mater. Today Proc. 24 (2020) 359–368, https://doi.org/10.1016/J.MATPR.2020.04.287.
[60] G.F. Shan, W. Yang, B.H. Xie, M.B. Yang, Mechanical properties and morphology of LDPE/PP blends, J. Macromol. Sci., Part B: Phys. 46 (2007) 963–974, https://doi.org/10.1080/00222340701457253.
[61] J.K. Palacios, A. Sangroniz, J.I. Eguiazabal, A. Etxeberria, A.J. Müller, Tailoring the properties of PP/PA6 nanostructured blends by the addition of nanosilica and compatibilizer agents, Eur. Polym. J. 85 (2016) 532–552.
[62] E. Karaagac, T. Koch, V.M. Archodoulaki, Choosing an effective compatibilizer for a virgin HDPE rich-HDPE/PP model blend, Polymers 13 (2021), https://doi.org/10.3390/POLYM13203567.
[63] B. Qiu, F. Chen, Y. Shangguan, L. Zhang, Y. Lin, Q. Zheng, Simultaneously enhancing strength and toughness for impact polypropylene copolymers by regulating the dispersed phase with high density polyethylene, RSC Adv. 4 (2014) 58999–59008, https://doi.org/10.1039/C4RA10682B.
[64] J. William, Impact Strength of Materials, Reprinted), Edward Arnold, London SE, 1983.